International Journal of Current Advanced Research
ISSN: O: 2319-6475, ISSN: P: 2319-6505, Impact Factor: SJIF: 5.995
Available Online at www.journalijcar.org
Volume 6; Issue 12; December 2017; Page No. 8421-8427
DOI: http://dx.doi.org/10.24327/ijcar.2017.8427.1358

Research Article

INVESTIGATION OF NEAR-INFRARED LUMINESCENCE PROPERTIES OF ER^{3+} DOPED DIFFERENT PHOSPHATE GLASSES FOR OPTICAL AMPLIFIER APPLICATIONS

Haritha B*., Damodaraiah S., Reddy Prasad V and Ratnakaram Y.C

Department of physics, S.V. University, Tirupati-517 502 A.P, India

A R T I C L E I N F O

Article History:
Received 29th September, 2017
Received in revised form 5th October, 2017
Accepted 3rd November, 2017
Published online 28th December, 2017

Key words:

Phosphate glass, Judd-Ofelt theory, 31P NMR, Photoluminescence, Decay profiles.

A B S T R A C T

Different phosphate glasses, $69.5P_2O_5$-$15Na_2CO_3$-$15MCO_3$ (M= Li, Mg, Ca and Ba) doped with 0.5 mol% erbium were prepared by melt quenching method. The spectroscopic and structural properties were characterized by X-ray diffraction, optical absorption, photoluminescence and solid state ^{31}P NMR techniques. Optical properties were characterized through optical absorption and emission spectra using Judd-Ofelt (J-O) theory. The J-O parameters were used to characterize the absorption and luminescence spectra of these glasses. From the theory, radiative properties like radiative transition probabilities (A_R), branching ratios (β_R) and radiative lifetimes (τ_R) of certain excited states have been evaluated for the fluorescent levels of Er^{3+} in these glasses matrices. The emission spectra in the NIR region show one transition i.e. $^4I_{13/2} \rightarrow {}^4I_{15/2}$ which is more intense. For this transition effective bandwidths ($\Delta\nu$) and emission cross sections (σ_p) have been evaluated. The decay curve analysis has been done for obtaining the decay constants of Er^{3+} for $^4I_{13/2}$ excited level in all the phosphate glasses. These results are compared with the literature and discussed. From the magnitudes of stimulated emission cross-sections and branching ratios certain glasses are suggested for laser applications.

Copyright©2017 ***Haritha B et al.*** *This is an open access article distributed under the Creative Commons Attribution License, which permits unrestricted use, distribution, and reproduction in any medium, provided the original work is properly cited.*

INTRODUCTION

Glasses doped with rare-earth ions have drawn much attention due to their potential applications in solid state lasers, optical amplifiers and three dimensional displays. Within various hosts, glasses are promising for optically active ions due to several reasons, for example selection of composition over a wide range, ease of fabrication in variety of shapes and sizes, allow relatively high doping levels, transparent over a wide optical range, less expensive etc. These glasses have broad absorption bands compared to the crystal hosts and so there is a high efficiency of absorption from broad band sources. Among various glasses phosphate based glasses are excellent materials due to their good chemical durability, ion-exchangeability, high gain coefficient and wide bandwidth capability. Also these phosphate glasses exhibit very important physical properties such as low melting temperature, low optical dispersion, high gain density, high solubility for RE oxides, high thermal expansion coefficient, low glass transition temperature, low softening temperature, low viscosity and high ultraviolet (UV) transmission, relatively high refractive indices and relatively low phonon energy which make them excellent applications in the industrial areas [1-3]. Phosphate based glasses have a wide range of potential applications in optical data transmission, detection, sensing and laser technologies due to their several special properties such as high transparency, high gain density, low melting temperatures and low optical dispersion [4-8].

The glasses doped with RE ions became superior to crystals because of several advantages such as easy preparation, large RE^{3+} ion doping capacity, large homogeneous line broadening etc. Glasses doped with RE ions are also playing a significant role in producing highly efficient up-conversion lasers. Among the rare earth ions, more attention have been paid on the Er^{3+} ion because of its favorable energy level structure has been exploited in a wide variety of glasses for applications in solid state lasers, micro chip lasers and optical amplifiers. In recent years wavelength division multiplexing (WDM) technology gained so much of attention as it increases the information carrying capacity of communication network used in telecommunication systems [9-10].

Erbium doped fiber amplifiers (EDFA) are used in the wavelength division multiplexing (WDM) system, eye safe lasers in medical fields [11]. This EDFA is one of the key divisions for use in 1.5 μm wavelength optical communication window. The broadening of optical communication window system becomes very important because of the rapid increase of information carrying capacity and the need of flexible networks [12]. Phosphate glasses are regarded as better hosts for Er^{3+} ions compared to the other glasses because of their

Corresponding author:* **Haritha B
Department of physics, S.V. University, Tirupati-517 502 A.P, India

higher phonon energy, more solubility of RE ions and smaller up-conversion of the $^4I_{3/2}$ level [13].

Recently Sreedhar *et al* [14] discussed luminescence studies on Er^{3+} doped zinc phosphate glasses for1.53µm laser applications. Amaranath Reddy *et al*. [15] discussed Er^{3+} doped phosphate glasses with improved gain characteristics for broad band optical amplifiers. Quennes *et al*. [16] investigated spectroscopic properties of Er^{3+} doped oxyfluoride glasses for photonic applications. Aroua Langer *et al*. [17] studied optical characterization and spectroscopic properties of Er^{3+} and Yb^{3+} doped phosphate borate glasses. Optical characterization of Er^{3+} doped zinc fluoro phosphate glasses for optical temperature sensors was reported by Vijaya *et al*. [18]. In the present work, vibrational modes and structural modes in the phosphate units are investigated using solid state NMR studies. Various spectroscopic parameters like radiative transition probabilities (A), radiative lifetimes (τ_R) and integrated absorption coefficients ($\sum$) are calculated from the absorption spectra of Er^{3+} doped different phosphate glasses using Judd-Ofelt theory. The laser characteristic parameters such as branching ratios (β) and stimulated emission cross-sections (σ_p) are obtained from emission spectra and are compared with other materials.

Experimental

In this study, the authors prepared and investigated four different Er^{3+} doped phosphate glasses using chemicals such as $NH_4H_2PO_4$, Na_2CO_3, Li_2CO_3, $BaCO_3$, $MgCO_3$, $CaCO_3$ and Er_2O_3. The method of preparation is a melt quenching method. All the chemicals are analar grade with 99.9% purity. Final glass compositions of the prepared glass samples were marked as follows.

1. $69.5NH_4H_2PO_4$ - 15N a_2CO_3 -15 Li_2CO_3 - $0.5Er_2O_3$
2. $69.5NH_4H_2$ PO_4 - 15 Na_2CO_3 -15$MgCO_3$ - $0.5Er_2O_3$
3. 3 .$69.5NH_4H_2PO_4$ - 15 Na_2CO_3 -15 $CaCO_3$ - $0.5Er_2O_3$
4. $69.5NH_4H_2$ PO_4 - 15N a_2CO_3 - 15 $BaCO_3$ - $0.5Er_2O_3$

The raw materials were thoroughly mixed in an agate motor and melted in an electric furnace at the temperature 950^0C–1000^0C for one hour in the porcelain crucible to obtain glass melt. The melt was quenched by pouring it on a preheated brass plate and pressed by another brass plate.

The obtained glasses were cooled at room temperature. The samples were polished before measuring their optical properties. The refractive index (n) measurements were performed using an Abbe's refractometer at sodium wavelength (589 nm) and these values are in the range 1.427–1.446 for glass matrices. The densities (d) of the glasses were calculated using Archimedes principle. The amorphous nature of the prepared Er^{3+} ion doped phosphate glasses were confirmed through the X-ray diffraction (XRD) studies using SIEFERT diffractometer employing Cu K_α radiation at 40 kV applied voltage and 30 mA anode current with a Si detector. The range of diffractometer is from 10^0 to 80^0 with step size of 0.02^0. SEM images were recorded using Carl Zeiss EVOMA15 Scanning Electron Microscope. Solid state NMR spectra were recorded to further study the structural evolution of prepared glasses using JEOL DELTA 2 NMR at 9.4T with a 4mm probe. The acquisition time was 18 ms and pulse width was 2.9 µs. The optical absorption spectral measurements were collected using a Varian Cary 5000 Spectrophotometer in UV-Vis region with 0.01 nm steps and in NIR region with 0.04 nm steps, with the resolution of <0.05 and <0.2 in the UV-Vis and the NIR regions respectively. The photoluminescence spectra and the decay curves of Er^{3+} doped glass samples were recorded using Jobin-Yvon Fluorolog 3 spectrofluorimeter (Horiba FL3-22iHR320). All these measurements were conducted at room temperature.

RESULTS AND DISCUSSION

x-ray diffraction, SEM analysis

Fig.1 shows the X-ray diffraction spectra of prepared glass samples. Absence of sharp peaks in the diffraction pattern confirms the amorphous nature of the glass matrices. Fig. 2 shows SEM image of Li glass matrix. The SEM image for Mg, Ca and Ba glasses were not shown, since all glass samples were found similar in nature. Fig. 2 shows no bubbles or crystals or clusters were observed in the bulk glass, which shows that the glass can be used for optical applications.

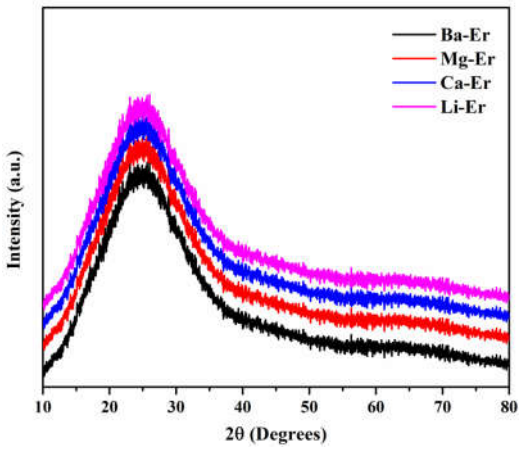

Fig 1 XRD profiles of 0.5 Mol % Er^{3+} doped different phosphate glasses.

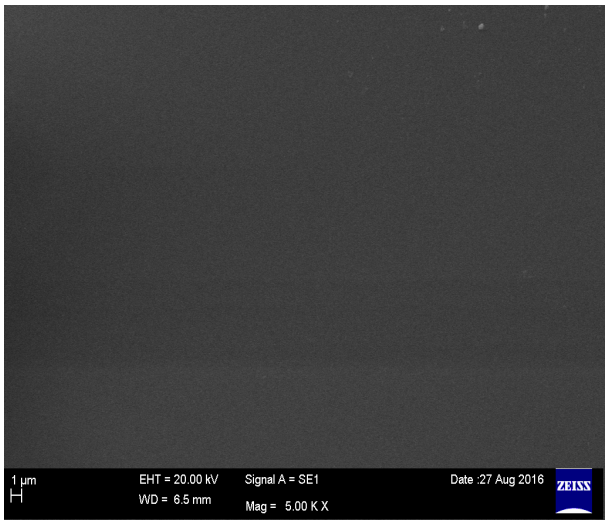

Fig 2 SEM image of Er^{3+} doped Li phosphate glass.

Fourier Transform Infrared Spectroscopy (FTIR)

The presence of functional and structural groups of prepared 0.5 mol% Er^{3+} doped different components of phosphate glass matrices are analyzed in the range 400–4000 cm^{-1} using transmission spectra, which are shown in Fig. 3. Several transmission bands are observed from infrared spectrum. Below are the results obtained from FTIR spectra regarding different bands and their assignments.

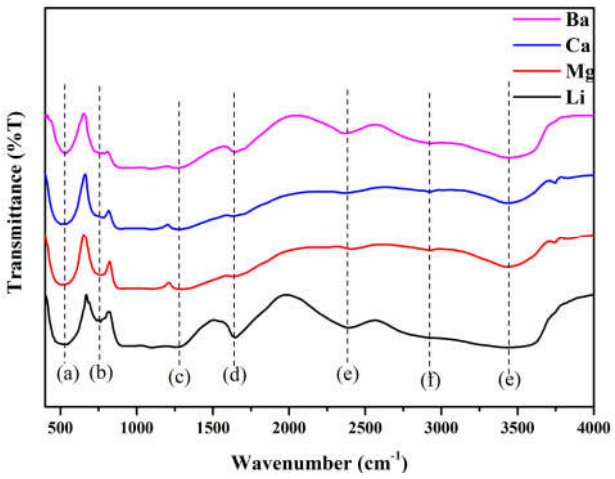

Fig 3 ^{31}P Solid state NMR Spectra of Er^{3+} doped different phosphate glasses.

1. The band at around ~529 cm^{-1} (a) is assigned to the bending mode of O–P–O in the Q^1 units [19].
2. The band at ~759 cm^{-1} (b) can be attributed to the symmetric stretching vibration of P–O–P rings (Q^2 species) [19].
3. The bands observed at about ~1258 (c), ~ 1636 cm^{-1}(d) are attributed to the asymmetric stretching of $(PO_2)^-$ in the Q^2 units [20].
4. The bands at around ~2386 (e), ~2916 cm^{-1} (f) are due to the hydrogen bonding [21].
5. The bands at around ~3450 cm^{-1} is due to symmetric stretching vibrations of hydroxyl groups (O–H) [22].

^{31}P NMR Spectroscopy

^{31}P Solid state NMR is a very important tool in characterizing structures of phosphate-type glasses due to the chemical shifts being sensitive to the phosphorus environment. The phosphate bonding is analysed through Q^n species, where the superscript n refers to the number of bridging oxygen's per tetrahedron. The soild state ^{31}P NMR spectra obtained for different glass matrices are shown in Fig.4.

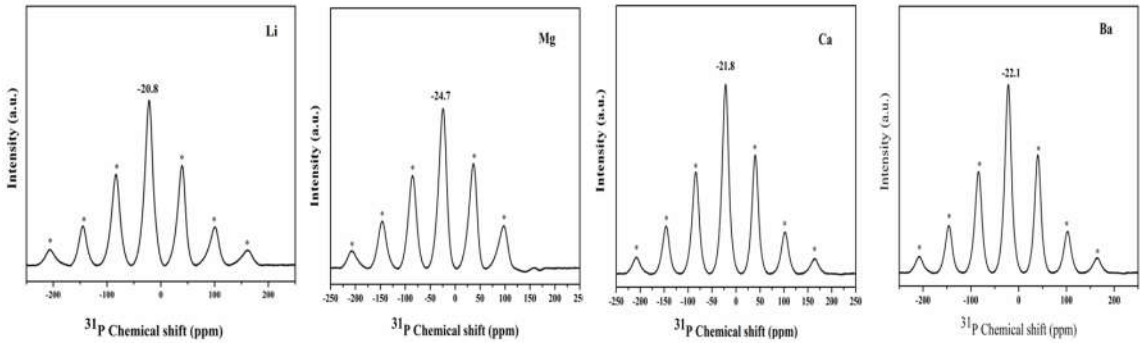

Fig 4 FT-IR spectra of Er^{3+} doped different phosphate glasses

It is noticed that Li, Mg, Ca and Ba phosphate glasses are exhibiting the signals with chemical shifts –20.8, -24.7, -21.8, -22.1 ppm respectively. These observed peaks of phosphate glass matrices are due to essentially of the Q^2 (meta phosphate) groups [23]. The signal has single symmetric Q^2 peak which indicates the existence of no other Q^0 (Phosphate tetrahedral with zero bridging oxygen's), Q^1 (Phosphate tetrahedral with one bridging oxygen's) and Q^3 (Phosphate tetrahedral with three bridging Oxygens) structural units.

Absorption spectra and Judd-Ofelt theory

When the glass host is doped with rare earth (RE) ion, the degenerate energy levels of the ions are split by the influence of Coulomb field and the overlapping of 4f electron shell with ligand shells. Optical absorption spectra are recorded in the wavelength range 350-700 nm at room temperature for all Er^{3+} doped phosphate glasses and are shown in Fig. 5. Similar absorption spectrum with same characteristics is observed in different other glasses doped with Er^{3+} ion [24-26]. From the figure, it is observed that various absorption transitions are observed from the ground state $^4I_{15/2}$ to the excited states $^4G_{11/2}$, $^2H_{9/2}$, $^4F_{7/2}$, $^2H_{11/2}$, $^4F_{9/2}$ and $^4I_{13/2}$. Among various absorption transitions, the transition $^4I_{15/2} \rightarrow {}^4F_{9/2}$ possesses higher intensity in the visible region centered at 15467 cm^{-1}. The observed band positions and their assignments of different absorption transitions of different phosphate glasses are presented in Table 1.

Table 1 Observed absorption bands along with their corresponding energies (cm^{-1}) of Er^{3+} doped different phosphate glasses.

Absorption band	Li	Mg	Ca	Ba
$^4G_{11/2}$	26596	26681	26631	26667
$^2H_{9/2}$	25608	25189	25031	25458
$^4F_{7/2}$	20640	20665	20631	20653
$^2H_{11/2}$	19313	19314	19313	19327
$^4F_{9/2}$	15468	15420	15432	15463
$^4I_{11/2}$	10300	10310	10363	10320
$^4I_{13/2}$	6551	6545	6552	6557

The optical absorption spectra are used to find the experimental spectral intensities for the observed bands and from that Judd-Ofelt intensity parameters (Ω_2, Ω_4, Ω_6) are obtained using the formulae given in Ref [27]. These parameters are important for the investigation of local structure and bonding in the vicinity of Er^{3+} ions. The intensity of absorption bands are measured by its spectral intensities which is related to the area under the absorption band. The experimental spectral intensities f_{exp} of different absorption bands of Er^{3+} doped different phosphate glasses are obtained using the formula given in Ref [28]. The calculated spectral intensities (f_{cal}) are obtained using the formula given in Ref [29]. Both f_{exp} and f_{cal} values of different absorption bands of Er^{3+} doped different phosphate glasses along with rms deviations are presented in the Table 2. The small rms deviation indicates that the calculation process is reliable between the experimental and theoretical values.

Among the three intensity parameters, Ω_2 is the most sensitive to the local structure and the glass composition which relates

to the degree of covalency of the RE-O bond and asymmetry around RE ions which in turn depends on the short range effects.

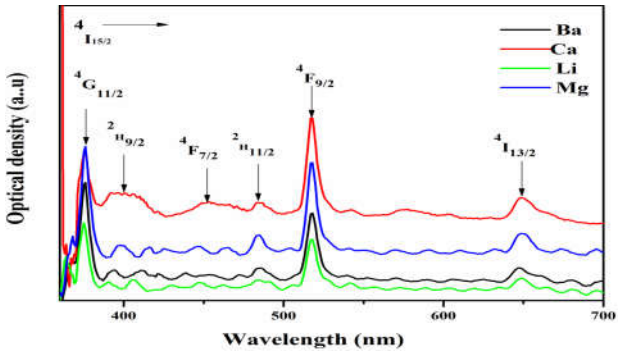

Fig 5 Optical absorption spectra of Er^{3+} doped different phosphate glasses.

Table 2 Experimental (f_{exp})and calculated(f_{cal}) spectral intensities ($f*10^{-6}$) of observed absorption bands of Er^{3+} doped different phosphate glasses.

absorption band $^4I_{15/2}\rightarrow$	Li		Mg		Ca		Ba	
	f_{exp}	f_{cal}	f_{exp}	f_{cal}	f_{exp}	f_{cal}	f_{exp}	f_{cal}
$^4G_{11/2}$	8.22	9.30	17.11	17.38	16.70	16.70	15.60	15.41
$^2H_{9/2}$	2.19	1.32	2.46	1.47	3.44	1.19	1.68	1.05
$^4F_{7/2}$	2.49	3.16	2.23	3.59	2.67	3.30	2.72	2.55
$^2H_{11/2}$	6.29	5.40	10.41	9.84	9.96	9.49	8.94	8.74
$^4F_{9/2}$	1.94	1.66	2.17	1.93	3.74	3.58	1.43	1.44
$^4I_{11/2}$	0.38	1.07	1.02	1.28	0.67	0.92	0.58	0.94
$^4I_{13/2}$	1.89	2.31	2.85	2.63	2.23	2.06	2.00	1.88
δ_{rms}	± 0.70		± 0.74		± 0.98		± 0.32	

The information related to the local structure surrounding the rare earth ions can be obtained by the analysis of Judd-Ofelt intensity parameters Ω (= 2, 4, 6) [30, 31]. The Ω_λ (λ=2, 4, 6) values are estimated based on best fitting calculations from the absorption data and the results are listed in the Table 3 along with those values obtained for other glasses matrices.

Table 3 Comparison of J-O parameters (Ω_λ *10^{-20} cm^2) and spectroscopic quality factors (X) of Er^{3+} doped in different host compositions

Glass	Ω_2	Ω_4	Ω_6	X	References
Li	2.03	1.19	0.14	0.11	Present work
Mg	4.02	1.81	0.63	0.34	Present work
Ca	3.07	1.72	0.16	0.09	Present work
Ba	3.55	1.80	0.27	0.15	Present work
KTFP	5.09	0.69	1.47	2.13	[32]
Flourphosphate	5.14	1.02	0.91	0.89	[33]
Fluoride	3.08	1.46	0.48	0.32	[34]
Germa-silicate	3.4	2.11	1.56	0.73	[35]

From the magnitude of Ω_2 parameter it is observed that the covalency is found to be in the order Mg>Ba>Ca>Li in these Er^{3+} doped phosphate glasses. Among all the phosphate glasses Mg has higher degree of covalency and Li glass has lower degree of covalency. For phosphate glasses covalency is decreased with respect to the radius of modifiers. As the radius of modifiers increases, the distance between the rare earth ions and oxygen increases and becomes less compact in nature and low coordination with oxygen ligand, hence covalency decreases. The low covalency of Li phosphate glass is due to the decrease of coordination between phosphate units and erbium ions through the oxygen i.e., P-O-Er. In the present work, Ω_2 in Mg glass is $4.02*10^{-20}$ cm which is higher than the bismuthate glasses [32].

In the present work the intensity parameters followed the trend in Li, Ba, Mg, Ca phosphate glasses is $\Omega_2>\Omega_4>\Omega_6$. Similar trend is observed in other reported glasses such as fluorphosphate [33], fluoride [34], KTFP [32], Germa-silicate [35] glasses. Among these three J-O parameters, Ω_4 has moderate influence and Ω_6 has least influence on the structure of the host matrix. The magnitude of Ω_4 and Ω_6 parameters depend on the bulk properties of the medium such as viscosity and dielectric constant of the media and these parameters were also affected by the vibronic transitions of the ions bounded to the ligand atoms [36, 37]. Ω_4 parameter is affected by the factors causing the changes of Ω_2 and Ω_6. Ω_6 parameter is higher in Mg phosphate glass matrix and lower in Li phosphate glass matrix indicating higher and lower rigidities and viscosities respectively.

Hyper sensitive transitions

The intensities of certain f-f transitions are larger compared to other transitions and are characterized by the higher values of

Table 4 Energies (cm^{-1}), electric dipole linestrengths (s_{ed} *$10^{20}/e^2$ cm^2), radiative transition probabilities (A_{ed}, s^{-1}), radiative branching ratios (β_R) and integrated absorption cross sections ($\sum*10^{18}$) for different excited states of Er^{3+} doped lithium phosphate glass.

Transition	ν	s_{ed}	A_{ed}	β_R	$\sum$
$^4G_{11/2}\rightarrow{}^2H_{9/2}$	987	71.41	0.2	0	0.1
$^4F_{3/2}$	4472	4.01	0.9	0	0.02
$^4F_{5/2}$	4415	5.57	1.2	0	0.03
$^4F_{7/2}$	5956	32.88	17.2	0.002	0.24
$^2H_{11/2}$	7283	18.78	18	0.002	0.16
$^4S_{3/2}$	8361	15.31	22.2	0.003	0.15
$^4F_{9/2}$	11128	91.53	312.4	0.043	1.23
$^4I_{9/2}$	14064	14.58	100.4	0.014	0.25
$^4I_{11/2}$	16296	6.01	64.4	0.009	0.12
$^4I_{13/2}$	20045	55.51	1107.3	0.152	1.34
$^4I_{15/2}$	26595	121.31	5651.4	0.775	3.88
$^4F_{5/2}\rightarrow{}^4F_{7/2}$	1541	22.85	0.4	0	0.08
$^2H_{11/2}$	2868	9.5	1.1	0.001	0.06
$^4S_{3/2}$	3946	1.85	0.6	0.001	0.02
$^4F_{9/2}$	6713	32.89	49.3	0.057	0.53
$^4I_{9/2}$	9649	11.12	49.5	0.057	0.26
$^4I_{11/2}$	11881	11.75	97.6	0.113	0.34
$^4I_{13/2}$	15630	26.14	494.4	0.574	0.98
$^4I_{15/2}$	22180	3.11	168.1	0.195	0.17
$^4F_{7/2}$->$^2H_{11/2}$	1327	33.07	0.3	0	0.08
$^4S_{3/2}$	2405	0.65	0	0	0
$^4F_{9/2}$	5172	7	3.6	0.002	0.07
$^4I_{9/2}$	8108	20.34	40.3	0.028	0.3
$^4I_{11/2}$	10340	34.38	141.2	0.097	0.64
$^4F_{13/2}$	14089	40.38	419.6	0.287	1.03
$^4I_{15/2}$	20639	26.21	856.1	0.586	0.98
$^2H_{11/2}$-->$^4S_{3/2}$	1078	23.96	0.1	0	0.04
$^4F_{9/2}$	3845	79.76	11.2	0.003	0.37
$^4I_{9/2}$	6781	51.33	39.6	0.011	0.42
$^4I_{11/2}$	9013	24.15	43.8	0.012	0.26
$^4I_{13/2}$	12762	12.8	65.9	0.018	0.2
$^4I_{15/2}$	19312	195.85	3493.6	0.956	4.55
$^4S_{3/2}$-->$^4F_{9/2}$	2767	0.33	0.1	0	0.01
$^4I_{9/2}$	5703	12.7	17.5	0.079	0.26
$^4I_{11/2}$	7935	1.63	6.1	0.028	0.05
$^4I_{13/2}$	11684	4.79	56.8	0.257	0.2
$^4I_{15/2}$	18234	3.12	140.5	0.636	0.21
$^4F_{9/2}$-->$^4I_{9/2}$	2936	25.78	1.9	0.002	0.11
$^4I_{11/2}$	5168	33.46	13.7	0.016	0.25
$^4I_{13/2}$	8917	21.61	45.5	0.053	0.28
$^4I_{15/2}$	15467	72.05	792.3	0.928	1.61
$^4I_{9/2}$-->$^4I_{11/2}$	2232	10.77	0.4	0.003	0.04
$^4I_{13/2}$	5981	11.04	7	0.059	0.1
$^4I_{15/2}$	12531	18.99	111	0.938	0.34
$^4I_{11/2}$->$^4I_{13/2}$	3749	42.32	5.5	0.154	0.19
$^4I_{15/2}$	10299	11.15	30.2	0.846	0.14
$^4I_{13/2}$--$^4I_{15/2}$	6550	37.96	22.6	1	0.26

reduced matrix element $\|U^2\|^2$. These transitions are known as hypersensitive transitions i.e., sensitive to the inhomogeneity of ligand environment and follows the selection rules $\Delta L \leq 2$, $\Delta J \leq 2$ and $\Delta S=0$ [38]. There are two hypersensitive transitions for Er^{3+} and they are $^4I_{15/2} \rightarrow {}^4G_{11/2}$ and $^4I_{15/2} \rightarrow {}^2H_{11/2}$. For these transitions the peak positions and the intensities are very sensitive to the environment of the rare earth ion. In the present work, it is observed that the intensities of the hypersensitive transitions $^4I_{15/2} \rightarrow {}^2H_{11/2}$ decrease with the decrease of Ω_2 parameter which is according to the theory and which is due to the strong interaction between 4f and 5d orbits [38]. In the present work it is observed that there is no shift of the peak wavelength of the hypersensitive transition for Li, Mg and Ca glass matrices, but for Ba glass matrix, there is a shift in peak wavelength of the hypersensitive transition.

Radiative and non-radiative Properties

Using the Judd-Ofelt intensity parameters (Ω_λ), electric dipole line strengths (S_{ed}), radiative lifetimes (τ_R), radiative transition probabilities (A_R), total transition probabilities(A_T), branching ratios(β_R) and integrated absorption cross-sections ($\sum$) for certain excited states of Er^{3+} doped different components of phosphate glasses are calculated and these values are presented in the Table 4 for Li glass matrix. Er^{3+} ion has many laser transitions such as $^4G_{11/2} \rightarrow {}^4I_{15/2}$, $^4F_{5/2} \rightarrow {}^4I_{15/2}$, $^4F_{7/2} \rightarrow {}^4I_{15/2}$, $^4S_{3/2} \rightarrow {}^4I_{15/2}$, $^4F_{9/2} \rightarrow {}^4I_{15/2}$ and $^4I_{13/2} \rightarrow {}^4I_{15/2}$. All these transitions terminate at the ground state level. Among various laser transitions $^4G_{11/2} \rightarrow {}^4I_{15/2}$ and $^4I_{13/2} \rightarrow {}^4I_{15/2}$ transitions are most important for laser action in the visible and NIR regions respectively. Radiative lifetimes, branching ratios and absorption cross-sections of certain excited states of Er^{3+} in different phosphate glass matrices are tabulated in Table 5.

In the present work, it was noted that the higher β_R, Σ values are observed in the Mg phosphate glass than other phosphate glass matrices for the transitions. Among all the excited states, $^4I_{13/2}$ state has higher radiative lifetimes for all phosphate glasses. Lower radiative lifetimes are observed for the excited state $^4G_{11/2}$ in all phosphate glasses. The branching ratio is a significant factor to any optical material, because it characterizes the possibilities of obtaining fluorescence from any specific transitions. Among different transitions, branching ratios of $^4I_{13/2} \rightarrow {}^4I_{15/2}$ transition is found to be the highest one. This transition may be useful for laser transition.

The exponential dependence of the multiphonon relaxation rate, W_{MPR}, on the energy gap to the lower level ΔE, has been experimentally established for a number of crystals and glasses and is given by [39]. This W_{MPR} is calculated using the formula given in the Ref [40] for the various excited states of Er^{3+} doped different phosphate glasses and is given in the Table 7.

Near infrared luminescence analysis

The infrared emission spectra of Er^{3+} doped different phosphate glasses are recorded in the 1400-1700nm wavelength region by exciting with 980 nm and are shown in figure 6 along with the energy level diagram. From energy level diagram it is observed that when Er^{3+} ions are excited with 980 nm, Er^{3+} ions in the ground state jumps to the $^4I_{11/2}$ state and then relax non-radiatively to the lower level $^4I_{13/2}$. Due to the longer lifetime (~ms) of this level, population inversion is achieved which enables the stimulated emission from the $^4I_{13/2}$ to $^4I_{15/2}$ (ground) state. From Fig. 5 it is observed that, maximum emission appears at 1534 nm for the $^4I_{13/2} \rightarrow {}^4I_{15/2}$ transition. The emission spectra of Er^{3+} doped different phosphate glass samples exhibit inhomogenous broadening in the range 1400-1700 nm. This band consists of both electric and magnetic dipole components, since it satisfies the selection rules $\Delta S = \Delta L = 0$, $\Delta J = +1$. The sharp peak observed at ~6423 and ~6512 cm^{-1} corresponds to the magnetic dipole transitions and broad peak observed at ~6293 and ~6657 cm^{-1} corresponds to the electric dipole transitions.

Table 5 Radiative lifetimes (τ_R in μs), branching ratio (β_R) and absorption cross sections ($\sum$)( ) of certain excited states of Er^{3+} doped different phosphate glass matrices.

Glass	$^4G_{11/2}$			$^4F_{5/2}$			$^4F_{7/2}$			$^4S_{3/2}$			$^4F_{9/2}$			$^4I_{11/2}$			$^4I_{13/2}$		
	τ_R	β_R	$\sum$	τ_R	β_R	$\sum$	τ_R	β_R	$\sum$	τ_R	β_R	$\sum$	τ_R	β_R	$\sum$	τ_R	β_R	$\sum$	τ_R	β_R	$\sum$
Li	137	0.772	3.88	1161	0.195	0.17	684	0.586	0.98	4529	0.636	0.21	1171	0.928	1.61	28011	0.846	0.14	44247	1	0.26
Mg	60	0.81	9.13	469	0.355	0.75	318	0.686	2.46	1051	0.665	0.92	647	0.917	2.88	8904	0.867	0.45	14104	1	0.80
Ca	96	0.767	5.47	860	0.165	0.19	484	0.556	1.31	3897	0.625	0.23	832	0.929	2.28	20576	0.84	0.18	34129	1	0.33
Ba	80	0.779	6.61	705	0.229	0.32	426	0.604	1.61	2384	0.646	0.40	754	0.925	2.49	15337	0.854	0.25	25002	1	0.45

Table 6 Peak wavelengths (λ_p (nm)), transition probabilities (A_R) (s^{-1}), measured and experimental branching ratios (β_R and β_{mes}), radiative lifetimes (τ_R) (μs), effective bandwidths (Δν) and peak stimulated emission cross section ($\sigma_{e*10}{}^{-21}$ cm^2) of $^4I_{13/2}$ of Er^{3+} doped different phosphate glasses

Transition	Parameters	Li	Mg	Ca	Ba
$^4I_{13/2} \rightarrow {}^4I_{15/2}$	λ_p(nm)	1533	1533	1533	1533.7
	$A_{R(}$ $s^{-1})$	22.6	70.9	29.3	39.9
	β_R	1	1	1	1
	β_{mes}	1	1	1	1
	T_{cal}	4.42	1.41	3.41	2.50
	T_{mes}	0.608	0.430	0.563	0.691
	Δν	245.3	239.1	250.5	202.8
	$\sigma_{e*10}{}^{-21}$ cm^2	1.200	3.950	1.600	2.590

Table 7 Multiphonon relaxation rates ($W_{MPR,}$ s^{-1}) of certain excited states of Er^{3+} ions doped different phosphate glasses.

Glass	$^4F_{7/2}$	$^2H_{11/2}$	$^4F_{9/2}$	$^4I_{11/2}$	$^4I_{13/2}$
Li	$2.92*10^{10}$	$1.35*10^{11}$	$6*10^7$	$1.01*10^6$	38.0
Mg	$2.90*10^{10}$	$1.26*10^{11}$	$5.89*10^7$	$1.45*10^6$	40.5
Ca	$2.93*10^{10}$	$1.43*10^{11}$	$5.15*10^7$	$1.20*10^6$	36.3
Ba	$2.97*10^{10}$	$1.57*10^{11}$	$5.5*10^7$	$2.10*10^6$	33.8

The effective bandwidth (Δν) in different phosphate glasses is found to be decreased in the order Ca<Li<Mg<Ba. The effective bandwidth in Mg phosphate glass is higher than the other phosphate glasses which suggest that inhomogeneous broadening is high in Ca phosphate glass. Lower homogeneous broadening is observed in Ba phosphate glass matrix. The difference in the effective bandwidths of Er^{3+} doped different phosphate glasses is due to the compositional differences. The stimulated emission cross sections (σ_p) of emission transition is one of the important parameters to identify a good optical material. A good optical material has higher emission cross section. In the present work, it is observed that the transition, $^4I_{13/2} \rightarrow {}^4I_{15/2}$ shows higher peak emission cross section i.e., 3.950 cm^2 in Mg glass among the four glass matrices. Its value is higher compared to the other glass matrices.

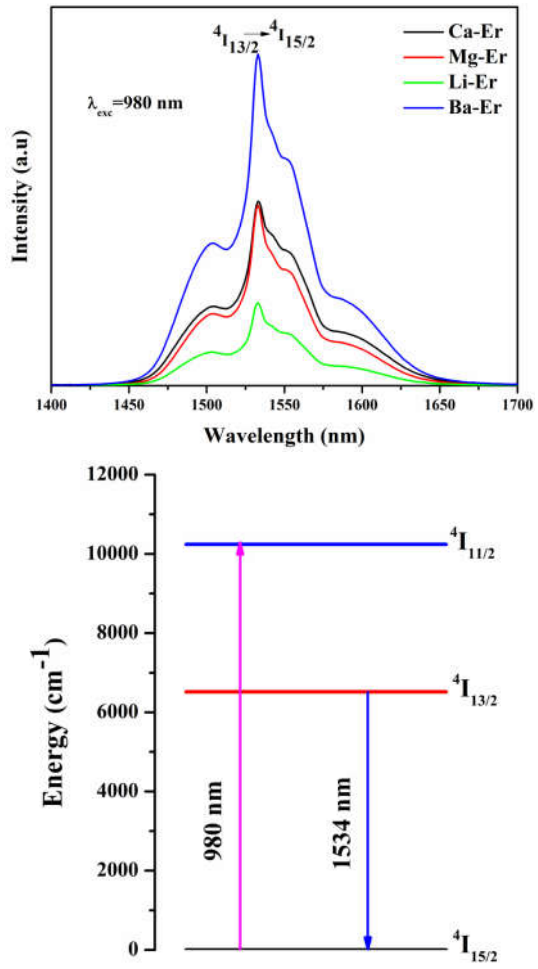

Fig 6 Emission spectra and energy level diagram of Er^{3+} doped different phosphate glasses.

Decay curve analysis

Fig. 7 shows decay curves of $^4I_{13/2}$ level of Er^{3+} ion in different phosphate glasses. These decay curves are measured by pumping 980 nm laser diode. All the curves are fitted to the bi-exponential function due to the hydrophilicity content of OH groups in phosphate glasses. The presence of the small traces of impurities (OH^-) or defects in the structure is likely to have impact on the decay levels. Lifetimes are determined to be 0.608, 0.430, 0.563 and 0.691 ms for Li, Mg, Ca and Ba contained Er_2O_3 doped glasses, respectively. The life time decay constants are estimated using the formulae given in Ref [40] and are presented in Table 6. From table, it is observed that the lifetime is higher for Ba glass and lower for Mg glass.

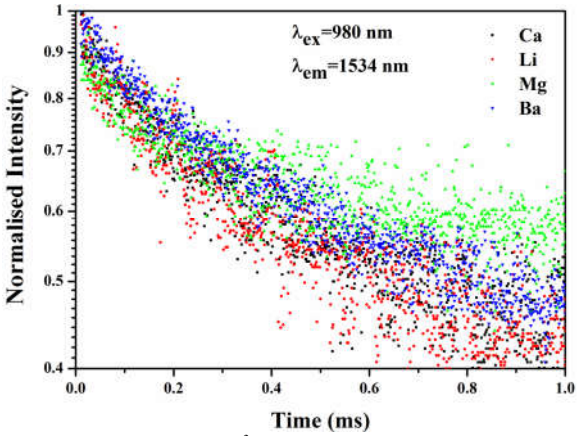

Fig 7 Decay profiles of Er^{3+} doped different phosphate glasses.

CONCLUSIONS

In the present work, Er^{3+} doped different phosphate glasses are prepared and characterized through various structural and spectroscopic measurements. X-ray diffraction patterns and SEM analysis reveal that the prepared glasses are amorphous in nature. On the basis of ^{31}P MAS NMR analysis, a decrease in the proportion of Q^2 units in the sequence Li-Ca-Ba-Mg in these different component host glasses was observed which indicates that these oxides are incorporated into the glass as network modifier oxides. From J-O analysis, Er^{3+} doped Mg phosphate glass environment has higher covalency and asymmetry than other three phosphate glasses. Higher radiative transition probability (A_R) is observed in the Mg phosphate glass than the other glasses matrices for the two transitions. Radiative lifetimes and branching ratios are higher than for the transition $^4I_{13/2}\rightarrow{}^4I_{15/2}$ than the other laser transitions. The transition $^4I_{13/2}\rightarrow{}^4I_{15/2}$ which is origin of 1.5µm NIR gives valuable information relating laser. The authors finally conclude that Mg doped phosphate glass is considered to be appropriate one for infrared laser and optical amplifier.

Acknowledgement

The authors acknowledge MoU-DAE-BRNS project (No.2009/34/36/BRNS/3174), Department of Physics, S.V. University, Tirupati, India for extending experimental facility.

References

1. G. Liebsh, I. Klimat, O.S. Wolfbeis, Advanced Materials, 11 (1999)1296-1299.
2. S.M. Borisov, O.S. Wolfbeis, Analytical Chemistry, 78 (2006) 5094-5101.
3. G.E. Khalil, K. Lau, G.D. Phelan, B. Carison, M. Gouterman, J.B. Cafllis, L.R. Dalton, Review of Scientific Instruments, 75(2004) 192-206.
4. S. Hraiech, M. Ferid, Y. Guyot, G. Bouton, *J. Rare Earth* 31 (2013) 685.
5. ET.Y. Lee, E.R.M. Taylor, *Opt. Mater*, 289 (2006) 200-206.
6. S. Tanabe, K. Hirao, N. Soga, *J. Non-Cryst. Solids* 122(1990)79-80
7. J.E. Pemberton, L. Latizahed, J.P. Fletcher, S.H. Risbud, *J. Chem. Mat.,* 3(1991)195
8. Hugo R. Fernades, Dilshat, U. Tulyaganov, Ashutosh goel, Manuel J. Ribeiro, T. Sorn, B. Karmakar, *Opt. Mat*., 31 (2009) 609-618.
9. T. Sornm B. Karmakar, Opt. Mat., 31 (2009) 609-618.
10. V.A.G.Rivera, S.P.A. Osorio, Y. Ledemi, D. Manzani, Y. Messaddeq, L.A. ONunes, E, Marege, Opt. Express 18(2010)25321-25328
11. L.R. Moorthy, M. Jayasimhadri, S.A. Saleem, D.V.R. Murthy, *J. Non-Cryst. Solids* 353 (2007) 1392.
12. Q. Qjah, C. Zhao, G.F. Yang, Z.M. Yang, Q.Y. Hang, Z.H. Jiang, Spectrochim. Acta Part A 71 (2008) 280.
13. H. Desirena, E.D. Rosa, L.A. Diaz-Torres, G.A. Kumar, *Opt. Mat*., 28 (2006) 560.
14. V.B. Sreedhar, N. Vijaya, D. Ramachari, C.K. Jayasankar, *Mol. Struct*., 1130 (2017) 1001-1008.
15. A. Amaranath Reddy, S. Surendra Babu, C. Vijaya Prakash, *Opt. Comm*., 285 (2012) 5354-5397.

16. K. Quennes, M.T. Soltana, M. Pou-lain, G. Bouloc, G. Alombert.-Gogec, Y. Guyot, A. Pillonnet, K. Lebbou, *J. Alloys compd.,* 603 (2014) 116-123.
17. Aroua Langer, Chaker Bouzidi, Habib, Elhouichet, M. *Ferid J. Lum*., 148 (2014) 249-255.
18. N. Vijaya, P. Babu, V. Venkatramu, C.K. Jayasankar, S.F. Leon-Luis, U.R. Rodriguez-Mendoza, L.R.Martin, V. Lavin Sensors and Actuators B 186 (2013) 156-164.
19. K. Selvaraju, K. Marimuthu, Physica B 407 (2012) 1086.
20. Meiqing Shi, Yanjie Lian, Liyuan Chai, Xiaobo Min, Zongwen Zhao, Shu Yang, *J. Molec. Struct*. 1081 (2015) 389–394.
21. Mingwei Lu, Fu Wang, Qilong Liao, Kuiru Chen, Jianfa Qin, Sheqi Pan, *J. Mol. Struct*. 1081 (2015) 187-192.
22. S. Selvi, G. Venkataiah, S. Arunkumar, G. Muralidharan, K. Marimuthu, Physica B 454 (2014) 72-81.
23. A. Marzouk, F.H. ElBatal, A.M. Abdelghany, Spectchim. *Acta Part* A 114 (2013) 658-667.
24. Sh. Liu, G. Zhao, Y. Li, H. Ying, J. Wang, G. Itan, *Opt. Mat*. 30 (2008) 1393.
25. B.R. Judd, *Phys. Rev*., 127 (1962) 750.
26. G.S. OFelt, *J. Chem. Phys*.37 (1962) 511.
27. S. Babu, A. Bala Krishna, D. Rajesh, Y.C. Ratnakaram, Spectrochim. *Acta part* A 22 (2014) 639.
28. S. Sunil Kumar, K. Jaya Krishna, S. Kasthuri Rangan, K.S.R. Koteswara Rao, K.P. Ramesh, *J. Non-Cryst. Solids* 357 (2011) 842-846.
29. J. Yang, S. Dai, Y. Zhou, L. Wen, L. Hu, Z. Jiang, *Appl. Phys.,* 93 (2003) 977-983.
30. H. Lin, E.Y.B. Pun, B. J. Chem. Y.Y. Zhang, *J. Appl. Phys*.103 (2008) 056103-056103-3.
31. S. Liu, G.g. Zhan, Y. Li, H. Ying, J. Wang, G. Hun, *Opt. Mat*., 30 (2008) 1393-1398.
32. Tao Wei, Fangze Chen, Ying Tian, X.U. Shiqing, *Opt. Comm*., 315 (2014) 199.
33. Y. Tian, R. Xu, L. Zhang, *Opt. Mat*., 34 (2011) 109.
34. L.R. Murthy, M. Jayasimhadri, S.A. Saleem, D.V.R. Murty, *J. Non-Cryst. Solids* 353 (2007) 1392.
35. H. Desirena, E.D. La Rosa, L.A. Diaz-Torres, G.A. Kumar, *Opt. Mat*., 28 (2006) 560.
36. P. Nachimuthu, R. Jagannatham, *J. Am. Ceram. Soc.,* 82 (1999) 387.
37. R. Reisfied, C.K. Jorgensen, Lasers and Excited States of Rare earths, Springer Verlag, New York (1975).
38. A. Majjane, A. Chahine, M. Et-tabirou, B. Echchahed, Trong-on Do, P.M.C. *Breen Mat. Chem. Phys*.143 (2014) 779-787.
39. M. Shojiya, M. Takashi, R. Kanno *et.al*, *J. Appl. Phys*., 82 (1997) 6259.
40. Huilong Guo, Jifu Bi, Jiayi wang, Xuequan zhang, shichun Jiang, Zhonghua wu, Dalton Trans. 44 (2015) 9130.

How to cite this article:

Haritha B *et al* (2017) 'Investigation of Near-Infrared Luminescence Properties of Er3+ Doped Different Phosphate Glasses for Optical Amplifier Applications', *International Journal of Current Advanced Research,* 06(12), pp. 8421-8427.
DOI: http://dx.doi.org/10.24327/ijcar.2017.8427.1358

****